Predator-informed looming stimulus experiments reveal how large filter feeding whales capture highly maneuverable forage fish

David E. Cade[a,1,2], Nicholas Carey[a,2,3], Paolo Domenici[b], Jean Potvin[c], and Jeremy A. Goldbogen[a]

[a]Hopkins Marine Station, Department of Biology, Stanford University, Pacific Grove, CA 93950; [b]Istituto per lo studio degli impatti Antropici e Sostenibilità in ambiente marino, Consiglio Nazionale delle Ricerche, IAS-CNR, 09170, Torregrande, Oristano, Italy; and [c]Department of Physics, Saint Louis University, St. Louis, MO 63103

Edited by James A. Estes, University of California, Santa Cruz, CA, and approved November 13, 2019 (received for review June 27, 2019)

The unique engulfment filtration strategy of microphagous rorqual whales has evolved relatively recently (<5 Ma) and exploits extreme predator/prey size ratios to overcome the maneuverability advantages of swarms of small prey, such as krill. Forage fish, in contrast, have been engaged in evolutionary arms races with their predators for more than 100 million years and have performance capabilities that suggest they should easily evade whale-sized predators, yet they are regularly hunted by some species of rorqual whales. To explore this phenomenon, we determined, in a laboratory setting, when individual anchovies initiated escape from virtually approaching whales, then used these results along with in situ humpback whale attack data to model how predator speed and engulfment timing affected capture rates. Anchovies were found to respond to approaching visual looming stimuli at expansion rates that give ample chance to escape from a sea lion-sized predator, but humpback whales could capture as much as 30–60% of a school at once because the increase in their apparent (visual) size does not cross their prey's response threshold until after rapid jaw expansion. Humpback whales are, thus, incentivized to delay engulfment until they are very close to a prey school, even if this results in higher hydrodynamic drag. This potential exaptation of a microphagous filter feeding strategy for fish foraging enables humpback whales to achieve 7× the energetic efficiency (per lunge) of krill foraging, allowing for flexible foraging strategies that may underlie their ecological success in fluctuating oceanic conditions.

predator/prey | looming stimulus | humpback whale | fish feeding | attack kinematics

In both terrestrial and aquatic ecosystems, maximum locomotor speed generally increases, but maneuverability decreases with increasing body sizes (1, 2). For pursuit predators chasing small prey at predator/prey size ratios of 10^0–10^1, this scaling property implies that speed advantages inherent in the predator's larger size can be counteracted by the prey's maneuverability advantages (2–4). At greater predator–prey size ratios (~10^2) that commonly occur in 3D, open ocean environments, whole-body acceleration attacks are generally suboptimal due to the maneuverability of the prey, and predators must use supplemental strategies, such as ambush, group coordination, or acceleration of smaller appendages to overcome their prey's escape abilities (2, 4, 5). As an alternate strategy for feeding on relatively small prey, some predators have evolved filter feeding mechanisms (6–8), but this high-drag foraging strategy is generally limited to slow and steady speeds and very large predator/prey size ratios >10^3 (7) where the size of the mouth counteracts the prey's maneuverability advantage. However, several medium-size rorqual species filter feed on small prey but can additionally target dense schools of forage fish, such as anchovies, sand lance, herring, and capelin at smaller predator/prey size ratios of 10^2 (9, 10). Fish of this size have the speed and maneuverability to quickly disperse if disturbed (Fig. 1*B* and Movie S1), and prior studies have found that prey are more likely to respond if approaching predators are large (11). The distance from the predator at which fish initiate an escape response (i.e., the reaction distance) is, thus, a critical factor in determining if an individual will escape an attack, and it follows that piscivorous filter feeding is only efficient for a large-bodied predator if it can attenuate the effectiveness of its prey's escape response; this study asks what mechanisms underlie a rapidly approaching whale's ability to avoid dispersing this potential energy source before it can be consumed.

Large filter feeding marine vertebrates that consume planktonic prey have evolved in several independent lineages of fishes and mammals (8) with most extant groups exhibiting slow and steady swimming speeds during foraging (7). In contrast, rorqual whales (a paraphyletic group within crown Balaenopteroidea) are unique in exhibiting a specialized lunge filter feeding strategy that is characterized by whole body acceleration and the intermittent and rapid engulfment of extremely large quantities of prey (6, 12). Among the largest animals of all time, rorquals range in size from 6 to 30 m, and all species exhibit at least part-time microphagy on krill (13) at a predator/prey length ratio on

Significance

Rorqual whales include the largest predators of all time, yet some species capture forage fish at speeds that barely exceed their quarry, suggesting that highly maneuverable fish should easily escape. We found that humpback whales delay the expansion of their jaws until very close to schools of anchovies, and it is only at this point that the prey react, when it is too late for a substantial portion of them to escape. This suggests that escape responses of these schooling fish, which have evolved under pressure from single-prey feeding predators for millions of years before the advent of lunge feeding, are not tuned sufficiently to respond to predators that can engulf entire schools, allowing humpback whales flexibility in prey choice.

Author contributions: D.E.C., N.C., P.D., and J.A.G. designed research; D.E.C., N.C., and P.D. performed research; D.E.C., N.C., P.D., and J.P. contributed new analytical tools; D.E.C., N.C., and P.D. analyzed data; J.A.G. administered the project and acquired funds; P.D. and J.A.G. supervised the project; P.D. and J.A.G. contributed substantially to manuscript drafts; and D.E.C. and N.C. wrote the paper.

The authors declare no competing interest.

This article is a PNAS Direct Submission.

Published under the PNAS license.

Data deposition: The data reported in this paper have been deposited in the Stanford Digital Repository, https://purl.stanford.edu/mt574ws5287.

[1]To whom correspondence may be addressed. Email: davecade@stanford.edu.

[2]D.E.C. and N.C. contributed equally to this work.

[3]Present address: Scottish Association for Marine Science, Oban, Argyll PA37 1QA, United Kingdom.

This article contains supporting information online at https://www.pnas.org/lookup/suppl/doi:10.1073/pnas.1911099116/-/DCSupplemental.

Downloaded at STANFORD UNIV MED CENTER on December 23, 2019

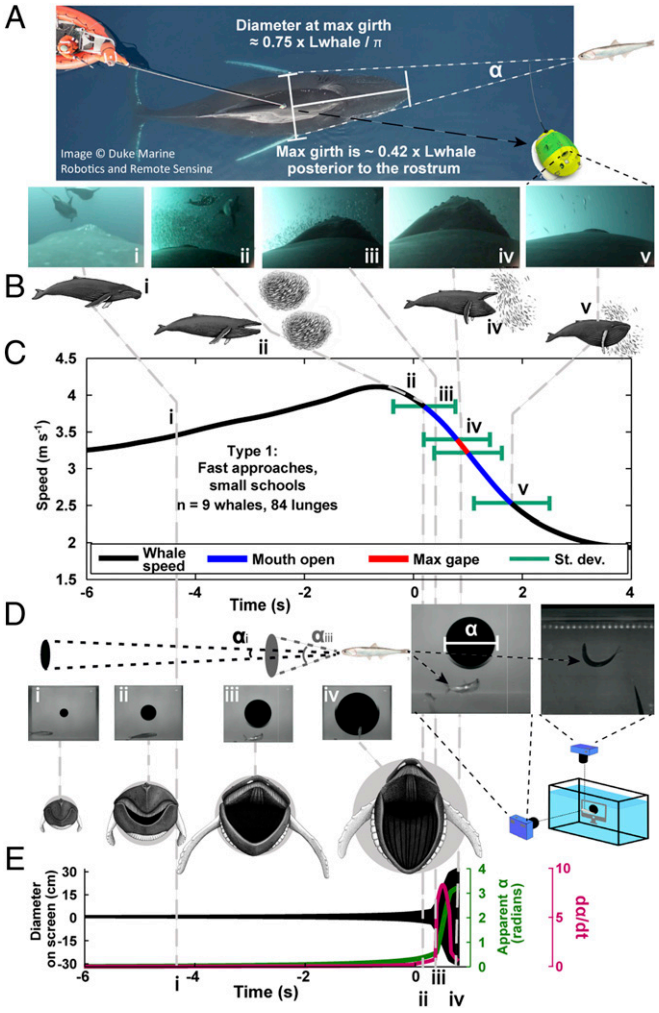

Fig. 1. This study combined field data, laboratory playbacks, and modeling. Points i–v are time aligned. (*A*) Suction cup video and 3D accelerometry tags were deployed on anchovy feeding (AF) humpback whales in California, USA. (*B*) Video recorded the behavior of schools as well as the timing of engulfment in relation to fish schools and to the whale's own acceleration profile. Fish did not break the school until the mouth opening (MO) event. (*C*) Mean speed profile of a Type 1 humpback whale. Lunge feeding is most efficient when engulfment coincides with deceleration. (*D*) Speed and engulfment were parameterized into looming stimuli and played back to anchovies in the laboratory. Anchovies demonstrated C-start escape responses at consistent thresholds of dα/dt. (*E*) Stimuli parameterized from predator data, as opposed to a constant approach speed, increased rapidly after the tips of the jaws were wider than the whale's maximum girth.

the order of 10^3. At these size differences, any prey maneuverability advantage is compensated for by the scale of the predator's mouth that would require prey to detect a threat from thousands of body lengths away and travel hundreds of body lengths per second to escape (2, 4). Indeed, when rorquals feed on krill, no escape response is observed (Movie S1). In contrast, some rorqual species hunt forage fish that are much more maneuverable than themselves and can actively escape (Movie S1), despite maximum lunge speeds that are the same or slower than for lunge feeding on krill (14). Hunting techniques that increase prey packing density, such as corralling and bubble netting have been noted in some rorqual species (15), but it has not been explained how an individual predator at this extreme body mass can, subsequently, accelerate toward a prey school without then dispersing the school.

Engulfment feeding on volumes of water that can exceed body mass is inherently an energetically costly endeavor (6, 16), and engulfment feeding on fish adds additional energetic costs as it commonly requires pursuit and aggregating maneuvers before engulfment. Additionally, while krill feeding (KF) whales use kinematically consistent and energetically efficient approach profiles, fish feeding whales use variable speeds and engulfment timings that can require higher energetic outputs since they involve continued body acceleration even after water starts to fill and expand the buccal cavity (14, 17). In this study, we sought to explain why fish feeding whales were less consistent in attack kinematics and posited that interactions between whales and maneuverable schooling prey played a role in modulating this behavior.

There is fossil evidence from freshwater deposits that schooling has existed as a fish behavior since, at least, 30–40 Ma earlier than when extreme gigantism arose in rorqual whales (18, 19). The transition to the age of giants was coincident with changes in oceanographic processes that encouraged upwelling and the formation of dense swarms of zooplankton (19). Although physical processes likely drive the aggregations of small-bodied plankton, forage fish aggregations are behaviorally mediated and likely evolved as a predator deterrent (20–22). It is, thus, likely that fish feeding whales benefit from the "rare enemy effect" (23) whereby the evolution of prey behavior, including the timing of their response to threats, has been driven by their more common encounters and long evolutionary history with predators that consume individual prey. We demonstrate how antipredator strategies related to schooling behaviors are, thus, counterproductive to avoiding large engulfment feeders.

Schooling in fish serves to intimidate or confuse predators targeting individual fish by either dissuading their attacks or making them less likely to succeed (5, 20–22). In contrast, a short-range flight response to a rapid predator approach manifests on an individual basis after a threshold of capture likelihood is passed. In both terrestrial and aquatic systems, there is pressure on individuals in an aggregation to not respond too early (24) as quick accelerations cannot only be energetically costly, jeopardizing future escape ability, but also leave the individual isolated from the group and much more vulnerable to predation (refs. 25 and 26 and Movie S1). The threshold of an observed predator approach at which prey respond is based on a combination of the size and speed of the predator (27–29). While fish can detect physical stimuli via the lateral line at very close proximity (~2 prey body lengths) (30, 31), fish in good visual conditions can detect approaching potential predators from much further away. Across taxa, potential prey have been shown to judge a potential predator's approach using some combination of the rate of change in the visual angle of a predator's outline (29, 32–34) and the apparent size of the approaching potential predator (27, 34–36). Escape responses of fish are, therefore, commonly investigated using visual looming stimuli to quantify the threshold at which escape decisions occur (Fig. 1 *D* and *E* and 27, 28, 33–38). Constant predator approach speeds are typically used to determine the specific range of looming thresholds (LTs) that stimulate escape responses (e.g., refs. 28, 34, and 38); in this study, we supplemented this technique by additionally exposing anchovies (*Engraulis mordax*) to looming stimuli directly parameterized on anchovy-feeding (AF) and KF humpback whale (*Megaptera novaeangliae*) speed and engulfment data collected from on-animal video biologging tags (14).

We used these looming stimulus experiments to determine the LTs at which individual anchovies responded to approaching predators in general, and humpback whales in particular. We subsequently collected additional field data from humpback whales attacking swimming schools of anchovies at high speed in Southern California (referred to throughout as Type 1 approaches) and contrasted those approaches with previously reported, relatively slow lunge feeding attacks (Type 2) on a relatively stationary

Downloaded at STANFORD UNIV MED CENTER on December 23, 2019

school of anchovies in Monterey Bay several times the size of the attacking whale (ref. 14 and Movie S2). We used mean data from both types of approaches and the experimentally derived LTs of anchovies to simulate how catch percentages would be affected by varying speed and engulfment profiles of the predator and calculated under what scenarios fish feeding whales would be incentivized to maximize catch percentage or, alternatively, to minimize the energetic cost of engulfment. Using this combination of field studies, laboratory experiments, and simulations (Fig. 1), we show how fish feeding humpback whales use not speed or maneuverability but stealth and deception (Fig. 2) to minimize and manipulate the escape responses of prey that have been evolving under pressure from particulate predators for millions of years before lunge feeding appeared as a strategy.

Results

Lunge Feeding Kinematics. The energetic costs of lunge feeding increase with increasing speed or if the whale accelerates against the increasing mass of engulfed water (Fig. 3). Therefore, lunge feeding involves biomechanically superfluous energetic costs if the onset of mouth opening (MO) does not coincide with peak speed: if MO is after peak speed, the whale uses energy to accelerate to higher speeds than necessary for engulfment, but if MO is before peak speed, the whale has to accelerate tons of engulfed water in addition to its own mass. Type 1, AF humpback whales (n = 9) reached maximum lunge speeds of 4.5 ± 0.8 m s^{-1} (mean ± SD) and were moving 3.8 ± 0.7 m s^{-1} at MO (95% confidence interval 0.5–1.0 m s^{-1} slower than peak) (Fig. 1*C*). MO varied considerably from peak speed (2.0 ± 2.4 s after) but was much more consistently related to a point of inflection in the speed profile before a period of rapid deceleration (0.2 ± 0.6 s after, *SI Appendix*, Fig. S3). In contrast, the Type 2 AF whale fed much more slowly (mean speed at engulfment: 2.2 ± 0.4 m s^{-1}, mean maximum speed: 2.5 ± 0.5 m s^{-1}), but also had highly variable MO times that averaged 1.1 ± 1.5 s before peak speed (Fig. 4*C*). Therefore, neither scenario displayed the cost-effective strategies of KF whales where engulfment initiation and peak speed coincide (14), implying that AF involves additional energetic costs.

Escape Responses of Anchovies. The perception of an approaching predator by a small fish can be represented as the angle (α) of the predator's maximum profile subtended on the retina of the prey (Fig. 1 *A* and *D*), and fish respond to the stimulus when the rate of change (dα/dt) of α crosses a species-specific threshold (32, 33) that may be modulated by the size of the stimulus (27, 34, 35). Using high-speed cameras, we recorded individual anchovies initiating escape responses to the constant speed approach of an expanding disk (Fig. 1*D* and Movie S3) at 1.66 ± 0.37 (range: 0.89–2.06 rad s^{-1}), a range that spanned 18 animation frames (300 ms). Other formulations of the response parameter that take into account both α and dα/dt were also calculated but did not better describe the observed variation in fish responses (see *SI Appendix*, Fig. S4 for a full discussion), so results presented here are for the simplest response model (a threshold of dα/dt) that retains high explanatory power. Since the stimulus response is triggered by the sensory system a few milliseconds before the fish makes a visible reaction (28), the range reported (referred to throughout as LT_{exp}) is the "true" LT after accounting for an estimated visual response latency of 61 ms. The visual response latency (range of 33–88 ms) was determined in separate experiments from the timing of anchovy escape responses to a bright flash and were comparable to visually mediated responses in other fish species (28, 37).

To determine how fish responded to actual predator approaches, we parameterized looming stimuli directly from KF and AF humpback whale speed and engulfment data (14) applied to a 10.5 m humpback whale (Fig. 1). Because the maximum diameter of the whale is located >4 m from its rostrum, in both the AF and the KF approaches, α increased slowly until a critical point during MO when the apparent angle of the jaw exceeded the apparent angle of the whale's maximum girth. At this apparent mouth opening (AMO) point, the widest part of the predator was instantaneously closer to the fish, was approaching near maximum speed, and was itself rapidly expanding as the whale's mouth approached maximum gape. All three of these factors combined to cause a rapid increase in α and a corresponding abrupt increase in dα/dt that encompassed the entire LT_{exp} range within a single animation frame (<17 ms) in both AF and KF playbacks (Fig. 1*E*, *SI Appendix*, Figs. S5 and S7, and Movie S3). Individual anchovies initiated escape between 30 and 270 ms after AMO (*SI Appendix*, Table S1 and Fig. S5) with responses to the AF playback (140 ± 80 ms after) not significantly different (P = 0.56) from responses to the KF playback (120 ± 80 ms after), implying that responses to KF and AF playbacks could not be further differentiated. Many of the escape responses occurred within the calculated visual latency range, but some were delayed up to an additional 180 ms (*SI Appendix*, Table S1), suggesting that for

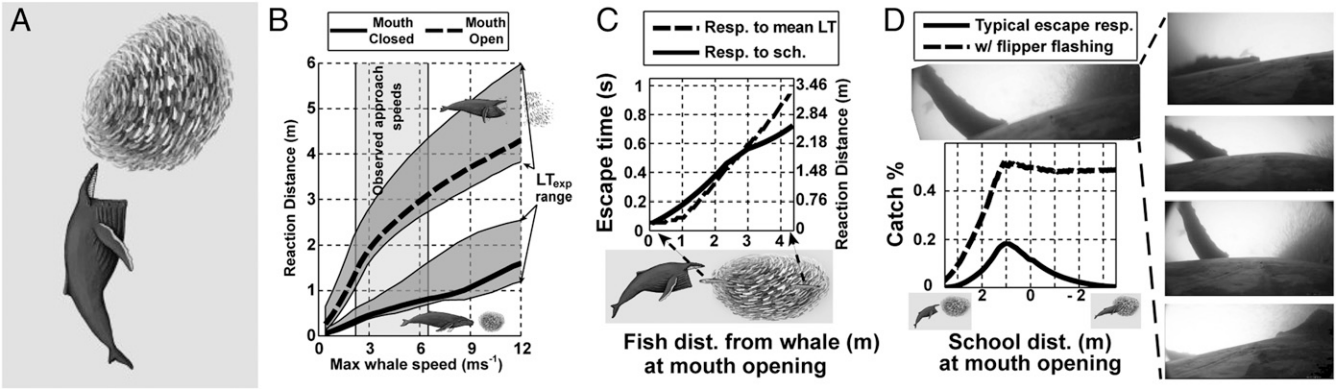

Fig. 2. Anchovies are evolutionarily conditioned to avoid small, fast, and mobile particulate feeding predators by forming and reacting as dense schools. Humpback whales, as less commonly encountered predators, take advantage of this strategy in 4 ways: (*A*) Lunge filter feeding enables engulfment of many individuals simultaneously. (*B*) MO close to the school results in shorter prey reaction distances equivalent to the whale's distance at apparent MO (AMO). This value will be intermediate between the 2 extremes of theoretical approaches (mouth always open and mouth always closed). (*C*) Anchovies at the back of a fleeing school will respond directly to the fish fleeing around it, however, these fish have less time to respond (resulting in a shorter reaction distance) than if they could see the approaching predator directly. (*D*) Humpback whale flippers can be 3 to 4 m in length—although not themselves used as weapons, they have white undersides that can be used to scare escaping fish back toward the school (see also Fig. 4 and Movie S4).

Downloaded at STANFORD UNIV MED CENTER on December 23, 2019

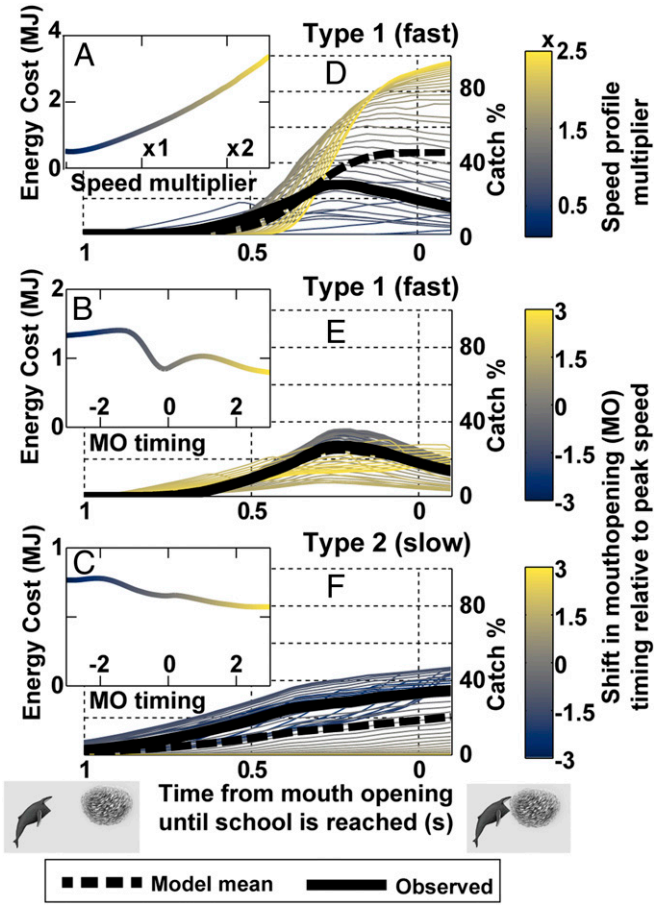

Fig. 3. Energy use during lunge feeding is a product of speed and engulfment timing, while catch percentage is a product of kinematics and the timing of engulfment with respect to the school. (*A*) Energy cost as speed of the mean fast humpback approach is varied. (*B*) Cost as the timing of MO relative to peak speed of the fast approach is varied. (*C*) Cost of varying MO timing for a slow approach. (*D*–*F*) How catch percentage varies both as a function of school distance at MO and with variation in speed (*D*) or MO timing (*E* and *F*). Thick black lines highlight the mean observed approaches.

some fish the abrupt increase in the stimulus at AMO may have been an unfamiliar threat requiring additional neural processing before the escape response was initiated. Crucially, a narrow temporal window around AMO of 34 ms spanned a dα/dt range (AF: 0.23–2.33, KF: 0.20–4.24 rad s^{-1}) that encompassed the entire range of true LT_{exp} and additionally maximized alternative response model forms that incorporated both α and dα/dt (*SI Appendix*, Fig. S4). The implication is that all fish, regardless of variation in response latency, respond very shortly after AMO. In 80 on-animal video observations of whale attacks on anchovy schools in situ, 67 showed the school dispersing closely following the observed MO (mean: 300 ± 360 ms after) with the earliest observed school dispersion occurring 400 ms before MO.

Video of whales approaching without opening their mouths (e.g., Movie S4) demonstrate that fish maintain school cohesion as the whale approaches, confirming our observation that the rapid expansion of the looming stimulus at AMO is likely responsible for initiating the anchovy escape response. If a whale, at typically observed attack speeds of ∼2–7 m s^{-1}, approaches without opening its mouth, it would be able to get within 1 m of the school before triggering a response (Fig. 2*B*). The substantial distance of the widest part of the (large) predator from the actual threat (the jaws) (Fig. 1*A*) serves to mask the distance of the approach until the jaws extend beyond the apparent profile and engulfment has already begun. The fundamental consequences of this are 1) delaying MO to be close to the school masks the threat of predation, and 2) faster approach speeds have a smaller effect on anchovy responses than does MO timing (Fig. 2), implying that faster approach speeds could increase capture rates since whales can better overcome prey escapes without startling their prey earlier.

Prey Capture Effectiveness under Different Engulfment Scenarios. We calculated when each individual fish in a school would escape from an approaching whale under different scenarios, assuming that fish would initiate escape responses at minimum, mean, or maximum LT_{exp} + 61 ms (a "quick response" using the estimated visual response latency) or + 261 ms (a "slow response" representative of the observed variation in response to AMO). Our models assume a visual stimulus since fish can likely perceive threats from a much further distance using vision than if relying on physical stimulus detection. That is, while there are no published data regarding the lateral line predator detection distance of schooling fish, adult fish, or any fish responding to a wave created from a whale-sized approaching object, our assumption that this distance is short is supported by previous research which has found that 1) lateral line detection of approaching predators in larval fish is <1.5 cm [1 to 2 prey body lengths (30, 31)], 2) lateral line detection of prey and neighboring fish is also 1 to 2 body lengths (39, 40), 3) the lateral lines of fish in motion are more than 3 orders of magnitude less sensitive than still fish (41), and 4) the lateral line in schooling fish is actively engaged in maintaining the school (42). Accordingly,

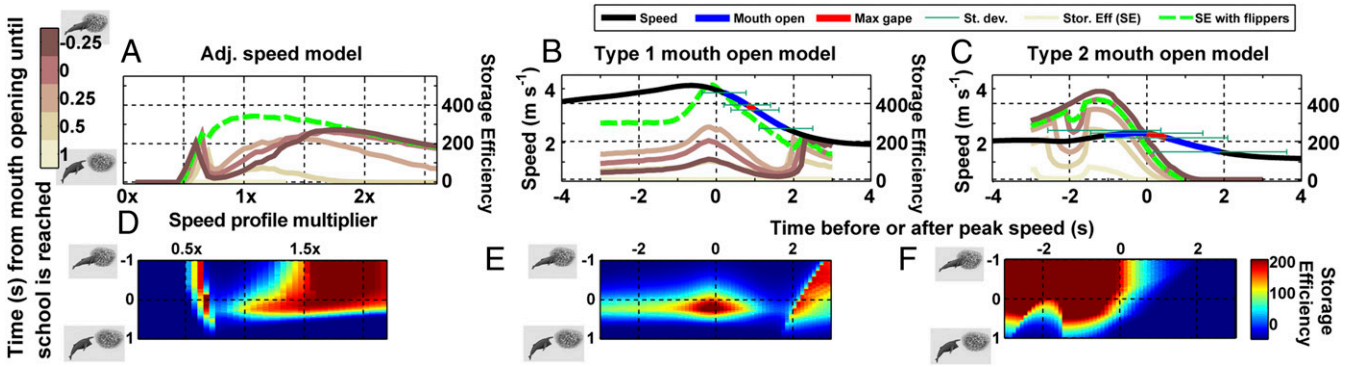

Fig. 4. Efficiency is affected by catch percentage and energy use as shown in Fig. 3. (*A*) At high speeds, efficiency drops sharply if whales open their mouths too early. Efficiency is increased for moderate speeds when the flippers are used to scare early fleeing fish back toward the mouth. (*B*) The timing of the MO in relation to the school has a much greater effect on efficiency than the timing in relation to peak speed. (*C*) At slow speeds, the timing of engulfment is less critical as efficiency can remain high.

Downloaded at STANFORD UNIV MED CENTER on December 23, 2019

results and discussion focus on simulations where the school is visually stimulated to respond at or before the whale reaches the school. Fish in the center of a school that cannot see the approaching whale directly do use the lateral line (in addition to vision) to initiate escape when others escape around them (40, 42); however, due to the time it takes a wave of response to pass through the school (*SI Appendix*), fish >2 m from the edge of the school actually have less time to escape than if they had been able to directly observe the oncoming predator (Fig. 2*C*).

For all simulations, we used a representative fish length of 12 cm and a school packing density of (1 body length)^3 per fish (*SI Appendix*) and assumed that the school was bigger than the engulfment volume of the whale. As predicted, prey capture is maximized when the whale begins MO close to the edge of the school (Fig. 3) and increases as the predator increases its speed (Fig. 3*A*). The cost of mistiming this event, however, is prodigious; in all scenarios, if the whale's mouth opens 1 s before reaching the school, the LT_{exp} is exceeded at a distance that allows every fish to escape. The increasing steepness of the slopes of the curves with speed (Fig. 3*A*) also demonstrates how precise timing becomes more important as speed increases. At slow speeds (Fig. 3*C* and *SI Appendix*, Fig. S1), catch percentage is maintained at ∼40% for a wide range of engulfment timings and does not increase substantially even in models with slow fish responses (*SI Appendix*, Fig. S1). In contrast, at faster speeds, if precise engulfment timing is obtained, the opportunity to catch more fish roughly doubles when fish are modeled to respond more slowly. Humpback whales also have a built-in buffer against early-responding fish; they are unique among cetaceans in having extraordinarily long flippers (∼30% of body length, see *SI Appendix*) with white undersides that they have been observed to rotate and extend during engulfment (ref. 43, Fig. 2*D*, and Movie S4) to expose fleeing prey to an additional stimulus that serves to turn fish back toward the school, increasing catch; this effect was most pronounced in models that assumed faster responses and faster speeds (*SI Appendix*, Fig. S2).

Foraging Efficiency. To examine how energetically efficient lunge feeding must balance energy intake (E_{in}) against locomotor costs (E_{out}, calculated from first principles; ref. 44), we defined the foraging efficiency as the *surplus efficiency*: the net energy gain from fish that would be captured proportional to the energy that would be spent: $(E_{in} - E_{out})/E_{out}$. Type 1 approaches, with more kinematic consistency, were used as a model to vary approach speed (which affected both E_{out} and E_{in}), and both approach types were used to model how distance from the school at MO (affecting E_{in}) and engulfment timing (affecting both E_{out} and E_{in}) influenced overall energetic gain.

A whale approaching a school using the Type 2 speed profile would use 68% more energy by doubling its speed and 275% more energy by quadrupling its speed. Energetic cost is minimal when MO is at peak speed or later (Fig. 3*A*) and maximal when the mouth is opened 1 to 2 s before peak speed as the whale must accelerate against increased drag from engulfment (Fig. 3 *B* and *C*). Accordingly, efficiency for the fast scenario peaked when the mouth opened coincident with engulfment and when the mouth opened exactly when the humpback reached the fish school (Fig. 4 *B* and *E*). Critically, particularly in faster scenarios if the whale mistimes its lunge in relation to the fish school, its efficiency drops more quickly than if it mistimes its engulfment in relation to acceleration (Fig. 4*E*). For example, if an approaching whale using a Type 1 profile opens its mouth 0.25 s before the fish school is reached, its efficiency would drop by 36%, but if it opens its mouth 0.25 s before peak speed, its efficiency drops by only 11%.

Comparisons with Other Predators. The attack model used to determine α and dα/dt at every point of approach (44) can also be parameterized with size and speed data from other predators. For an AF particulate predator, the California sea lion (*Zalophus californianus*), the mean LT_{exp} for an anchovy would be exceeded by ∼0.5 m before the fish is reached (*SI Appendix*, Fig. S7), allowing it to escape a distance (6.6 cm) that is greater than the width of a sea lion jaw (*SI Appendix*) and implying that the sea lion (predator/prey size ratio ∼10^1) must rely on its noted maneuverability (45) to be successful. When the stimulus is parameterized with blue whale size and attack data, similar to humpback whales, mean LT_{exp} is not reached until AMO. Due to the long engulfment duration of blue whales (14), however, AMO is still 1.2 s and 2.8 m before the mouth even finishes opening. Due to the consequent increased time to escape, <15% of fish would be caught (*SI Appendix*, Fig. S7*B*), potentially explaining why blue whales are known to be almost exclusively euphausivores (13).

In prior experiments with other species, it has been suggested that an individual's response to a specific LT is progressively inhibited at larger stimulus sizes (27, 34, 35). That is, individuals would be less likely to respond at the same values of dα/dt if the object is closer, or, as in this unique case, substantially larger. This would imply that humpback whales have an inherent advantage over smaller predators: At any given distance from the prey, they would appear much larger than a smaller predator, and, at any given α, α will be increasing more slowly since the whale would be further away. Applying a response model that incorporates α inhibition (η in ref. 35, see *SI Appendix*, Fig. S4) results in an increased catch of 30% above the dα/dt threshold model in Type 1 approaches and no increase in Type 2 approaches (*SI Appendix*, Fig. S1).

Discussion

For predator/prey size ratios of 10^0–10^1, the speed of a predator can overcome the maneuverability of prey when $v > \sqrt{r}$, where v is the ratio of predator speed to prey speed and r is the ratio of turning radii (a measure of maneuverability) (2–4). At predator/prey size ratios of 10^2, the size ratio of humpbacks feeding on fish, r is also 10^2, and a predator would have to be more than 10 times as fast as its prey to overcome its maneuverability disadvantage. In contrast, we observed that the average humpback whale speed at MO of 3.8 m s^{-1} [with even slower attack speeds also reported (14, 46)] was only 60% higher than mean anchovy escape speeds (*SI Appendix*, Fig. S6) and decreased rapidly throughout the lunge, implying that these predators should not theoretically be able to capture fish.

If a group of small fish is treated as a unit, however, the predator/prey size ratio for humpback whales and anchovy schools is decreased to 10^1. Humpback whales in this study pursuing anchovies in concert with common dolphins (Movie S2) sustained speeds of up to 6 m s^{-1} for up to a minute before slowing down on the final approach to a lunge. The speed of an anchovy school is likely no greater than an individual anchovy's maximum sustained swimming speed of 60 cm s^{-1} (47)—about 10 times slower than the observed humpback whale speeds—implying that, on approach, these whales overcome the $v = \sqrt{r}$ restriction and providing an additional rationale for high speeds of attack despite the increased precision in engulfment timing required. Once an imminent, individual threat is perceived by the prey, however, an individual prey escape response is initiated whereby burst speeds combined with individual maneuverability become the dominant escape mechanisms and the school disperses. Anchovies have the performance capabilities to evade capture if they respond to a threat with sufficient time; our simulations suggest that, if the LT of response was reduced (i.e., anchovies were more sensitive to threats) to 0.5 rad s^{-1}, 97% of fish would escape since they would begin to flee

Downloaded at STANFORD UNIV MED CENTER on December 23, 2019

earlier, and if LT was reduced to 0.3 rad s^{-1}, 99.8% of fish would escape. These results explain how whales catch fish despite the capabilities of their prey to escape by delaying the moment at which individual fish perceive the threat. It should additionally be noted that the initiation of individual escape responses in situ may be further delayed from what we found in the laboratory since, in natural settings, existence within a large group often inhibits individual flight responses due to the risk dilution effect in concert with direct occlusion of the stimulus (34, 48). This conserved behavioral feature is safer for an individual when it is targeted by predators hunting single fish but is counterproductive when the school itself is in danger of predation and, as such, may further serve to increase the captured proportion of a school, resulting in catches closer to the slow response scenarios (*SI Appendix*, Figs. S1 and S2).

We found that efficiency is dominated more by catch percentage than by the energetic cost of a lunge (Fig. 4). Therefore, the most important factor that will increase foraging efficiency in engulfment filter feeders is the maintenance of packing density within the school. Small prey, such as krill and copepods, form large aggregations generally through passive processes, such as advection (49). Forage fish, in contrast, form schools actively and often explicitly as antipredation strategies (20–22). Humpback whales in many populations worldwide utilize a variety of strategies for inducing schooling fish into tighter aggregations including foraging in concert with particulate feeding predators (50) or by physically (15) or acoustically (51, 52) manipulating prey into tighter aggregations. The humpback whales in this study foraged by following common dolphins (*Delphinus sp.*) that herd fish into tighter schools or in concert with groups of California sea lions (Movie S2). However, these schools scattered into smaller highly maneuverable units during engulfment events (Movie S1), implying that the success of humpback whale foraging depends on delaying this scattering response. Our results support this analysis whereby whales use their bulk to hide in plain sight: Even though they are visible to individual anchovies on the outside of a school, they do not appear to be a threat since their visual approach profile does not reach anchovies' LT before they open their mouths and begin engulfment, at which point it is too late for a substantial portion to disperse. The paradoxical increased risk to individuals that results from staying with the school instead of dispersing early likely results from forage fish fine-tuning visual response thresholds over evolutionary timescales for particulate feeding predators—a threat for which it is safer for each individual to stay in the school (26). This strategy, however, is not effective for avoiding predation by a lunge feeding whale of extreme size that can engulf a large portion of a school simultaneously.

Schools of anchovies are highly mobile, and, consequently, the overall feeding rates we observed were substantially lower (3.9 ± 2.0 lunges h^{-1}) than for California KF whales (23.0 ± 17.9 lunges h^{-1}). Over long timescales, it is, thus, only efficient to forage on fish if the energy intake from individual feeding events is higher than for KF events. Indeed, we found that an AF whale catching 40% of a school would get 6.8 times more energy per lunge than a KF whale (see the details in the *SI Appendix*). Additionally, the locomotor cost of AF is also higher than for KF. Likely because prey escape is a minimal consideration during KF (e.g., Movie S1), these whales appear to adopt the most hydrodynamically efficient engulfment profiles where MO coincides with maximum speed (14). In contrast, AF humpback whales, which, like other animals that perform banking turns (53), can use their flippers to increase maneuverability at higher speeds (54) and make fine-scale adjustments in attack speed and body orientation that facilitate the onset of engulfment as close as possible to the fish school, even if that means accelerating against the drag of an open mouth (Fig. 4). The surprisingly energetically costly engulfment profiles previously noted for fish feeding whales (14, 17) can, thus, be explained by the need to time engulfment to be proximal to the fish school, thereby maximizing energy intake (Fig. 4).

High-speed engulfment filter feeding by large predators is a relatively recent evolutionary phenomenon; it is likely that rorqual whales evolved this feeding modality from an ancestral raptorial suction feeding state to take advantage of upwelling-induced zooplankton patchiness that appears to have become more readily available in the late Miocene (19). Forage fish, such as anchovies, however, have likely been under attack from a variety of single-prey feeding predators for hundreds of millions of years. In contrast to larger baleen whale species that specialize on zooplankton, we suggest that the large size of humpback whales has allowed them to exapt their unique lunge filter feeding mechanism to exploit some aspects of the antipredator defenses of anchovies, allowing them to feed on a greater variety of prey. Consequently, the enhanced foraging flexibility resulting from this generalist strategy has likely contributed to the humpback whale's ability to recover from 20th century near extermination (55) and might continue to make them less vulnerable to future climatic-induced ecosystem changes than more specialist and more endangered ocean giants (56).

Data Availability. R and Matlab code to calculate the diameter of the looming stimulus and the energetic cost of a lunge is available at https://purl.stanford.edu/mt574ws5287 (44).

ACKNOWLEDGMENTS. Special thanks to John Calambokidis, Ari Friedlaender, and David Johnston and the crew of the Research Vessel Truth for spearheading field operations; to Jo Welsh for anchovy specimens; to Madison Bashford, Ben Burford, and Diana Li for experimental assistance; to Jake Linsky for analytical assistance; to Jessica Bender for sea lion illustrations; and to Alex Boersma for the remainder of the illustrations. Thanks should be extended to the three anonymous reviewers whose careful considerations strengthened the manuscript. This work was funded with NSF Integrative Organismal Systems Grant 1656691, Office of Naval Research Young Investigator Program Grant N000141612477, and Stanford University's Terman and Bass Fellowships. All procedures were conducted under institutional Institutional Animal Care and Use Committee guidelines and National Marine Fisheries Service permit 16111.

1. R. P. Wilson *et al.*, Mass enhances speed but diminishes turn capacity in terrestrial pursuit predators. *eLife* **4**, e06487 (2015).
2. P. Domenici, The scaling of locomotor performance in predator-prey encounters: From fish to killer whales. *Comp. Biochem. Physiol. A Mol. Integr. Physiol.* **131**, 169–182 (2001).
3. H. C. Howland, Optimal strategies for predator avoidance: The relative importance of speed and manoeuvrability. *J. Theor. Biol.* **47**, 333–350 (1974).
4. P. W. Webb, V. De Buffrénil, Locomotion in the biology of large aquatic vertebrates. *Trans. Am. Fish. Soc.* **119**, 629–641 (1990).
5. P. Domenici *et al.*, How sailfish use their bills to capture schooling prey. *Proc. R. Soc. B: Biol. Sci.* **281**, 20140444 (2014).
6. J. A. Goldbogen *et al.*, How baleen whales feed: The biomechanics of engulfment and filtration. *Annu. Rev. Mar. Sci.* **9**, 367–386 (2017).
7. M. Simon, M. Johnson, P. Tyack, P. T. Madsen, Behaviour and kinematics of continuous ram filtration in bowhead whales (Balaena mysticetus). *Proc. R.Soc.B. Biol. Sci.* **276**, 3819–3828 (2009).
8. M. Friedman *et al.*, 100-million-year dynasty of giant planktivorous bony fishes in the Mesozoic seas. *Science* **327**, 990–993 (2010).
9. A. H. Fleming, C. T. Clark, J. Calambokidis, J. Barlow, Humpback whale diets respond to variance in ocean climate and ecosystem conditions in the California current. *Glob. Change Biol.* **22**, 1214–1224 (2016).
10. D. L. Wright, B. Witteveen, K. Wynne, L. Horstmann-Dehn, Evidence of two subaggregations of humpback whales on the Kodiak, Alaska, feeding ground revealed from stable isotope analysis. *Mar. Mamm. Sci.* **31**, 1378–1400 (2015).
11. W. E. Cooper, Jr, T. Stankowich, Prey or predator? Body size of an approaching animal affects decisions to attack or escape. *Behav. Ecol.* **21**, 1278–1284 (2010).
12. P. Brodie, Cetacean energetics, an overview of intraspecific size variation. *Ecology* **56**, 152–161 (1975).
13. A. Kawamura, A review of food of balaenopterid whales. *Sci. Rep. Whales Res. Inst.* **32**, 155–197 (1980).
14. D. E. Cade, A. S. Friedlaender, J. Calambokidis, J. A. Goldbogen, Kinematic diversity in rorqual whale feeding mechanisms. *Curr. Biol.* **26**, 2617–2624 (2016).
15. D. Wiley *et al.*, Underwater components of humpback whale bubble-net feeding behavior. *Behaviour* **148**, 575–602 (2011).
16. A. Acevedo-Gutiérrez, D. A. Croll, B. R. Tershy, High feeding costs limit dive time in the largest whales. *J. Exp. Biol.* **205**, 1747–1753 (2002).

Downloaded at STANFORD UNIV MED CENTER on December 23, 2019

17. M. Simon, M. Johnson, P. T. Madsen, Keeping momentum with a mouthful of water: Behavior and kinematics of humpback whale lunge feeding. *J. Exp. Biol.* **215**, 3786–3798 (2012).
18. N. Mizumoto, S. Miyata, S. C. Pratt, Inferring collective behaviour from a fossilized fish shoal. *Proc. Biol. Sci.* **286**, 20190891 (2019).
19. G. J. Slater, J. A. Goldbogen, N. D. Pyenson, Independent evolution of baleen whale gigantism linked to Plio-Pleistocene ocean dynamics. *Proc. Biol. Sci.* **284**, 20170546 (2017).
20. J. Krause, G. D. Ruxton, *Living in Groups* (Oxford University Press, 2002).
21. J.-G. J. Godin, Antipredator function of shoaling in teleost fishes: A selective review. *Nat. Can.* **113**, 241–250 (1986).
22. A. E. Magurran, The adaptive significance of schooling as an anti-predator defence in fish. *Ann. Zool. Fenn.* **27**, 51–66 (1990).
23. R. Dawkins, *The Extended Phenotype: The Gene as the Unit of Selection* (Freeman, ed. 1982, 1982).
24. R. C. Ydenberg, L. M. Dill, The economics of fleeing from predators. *Adv. Study Behav.* **16**, 229–249 (1986).
25. A. E. Magurran, T. J. Pitcher, Provenance, shoal size and the sociobiology of predator-evasion behaviour in minnow shoals. *Proc. R. Soc. Lond. B Biol. Sci.* **229**, 439–465 (1987).
26. C. C. Ioannou, F. Rocque, J. E. Herbert-Read, C. Duffield, J. A. Firth, Predators attacking virtual prey reveal the costs and benefits of leadership. *Proc. Natl. Acad. Sci.* **116**, 8925–8930 (2019).
27. N. Hatsopoulos, F. Gabbiani, G. Laurent, Elementary computation of object approach by wide-field visual neuron. *Science* **270**, 1000–1003 (1995).
28. A. Paglianti, P. Domenici, The effect of size on the timing of visually mediated escape behaviour in staghorn sculpin *Leptocottus armatus*. *J. Fish Biol.* **68**, 1177–1191 (2006).
29. P. W. Webb, Avoidance responses of fathead minnow to strikes by four teleost predators. *J. Comp. Physiol.* **147**, 371–378 (1982).
30. W. J. Stewart, G. S. Cardenas, M. J. McHenry, Zebrafish larvae evade predators by sensing water flow. *J. Exp. Biol.* **216**, 388–398 (2013).
31. M. J. McHenry, K. E. Feitl, J. A. Strother, W. J. Van Trump, Larval zebrafish rapidly sense the water flow of a predator's strike. *Biol. Lett.* **5**, 477–479 (2009).
32. P. Domenici, The visually mediated escape response in fish: Predicting prey responsiveness and the locomotor behaviour of predators and prey. *Mar. Freshwat. Behav. Physiol*. **35**, 87–110 (2002).
33. L. M. Dill, The escape response of the zebra danio (Brachydanio rerio) I. The stimulus for escape. *Anim. Behav.* **22**, 711–722 (1974).
34. A. M. Hein, M. A. Gil, C. R. Twomey, I. D. Couzin, S. A. Levin, Conserved behavioral circuits govern high-speed decision-making in wild fish shoals. *Proc. Natl. Acad. Sci. U.S.A.* **115**, 12224–12228 (2018).
35. T. Preuss, P. E. Osei-Bonsu, S. A. Weiss, C. Wang, D. S. Faber, Neural representation of object approach in a decision-making motor circuit. *J. Neurosci.* **26**, 3454–3464 (2006).
36. I. Temizer, J. C. Donovan, H. Baier, J. L. Semmelhack, A visual pathway for looming-evoked escape in larval zebrafish. *Curr. Biol.* **25**, 1823–1834 (2015).
37. R. Batty, Escape responses of herring larvae to visual stimuli. *J. Mar. Biol. Assoc. U. K.* **69**, 647–654 (1989).
38. C. K. Faulk, L. A. Fuiman, P. Thomas, Parental exposure to ortho, para-dichlorodiphenyltrichloroethane impairs survival skills of Atlantic croaker (*Micropogonias undulatus*) larvae. *Environ. Toxicol. Chem.* **18**, 254–262 (1999).
39. J. Montgomery, R. Milton, Use of the lateral line for feeding in the torrentfish (Cheimarrichthys fosteri). *N. Z. J. Zool.* **20**, 121–125 (1993).
40. E. J. Denton, J. Gray, Mechanical factors in the excitation of clupeid lateral lines. *Proc. R. Soc. Lond. B Biol. Sci.* **218**, 1–26 (1983).
41. I. Russell, B. Roberts, Active reduction of lateral-line sensitivity in swimming dogfish. *J. Comp. Physiol.***94**, 7–15 (1974).
42. K. Faucher, E. Parmentier, C. Becco, N. Vandewalle, P. Vandewalle, Fish lateral system is required for accurate control of shoaling behaviour. *Anim. Behav.* **79**, 679–687 (2010).
43. M. M. Kosma, A. J. Werth, A. R. Szabo, J. M. Straley, Pectoral herding: An innovative tactic for humpback whale foraging. *R. Soc. Open Sci.* **6**, 191104 (2019).
44. D. E. Cade, N. Carey, P. Domenici, J. Potvin, J. A. Goldbogen, Predator-informed looming stimulus experiments reveal how large filter feeding whales capture highly maneuverable forage fish. Stanford Digital Repository. https://purl.stanford.edu/mt574ws5287. Deposited 11 October 2019.
45. F. E. Fish, J. Hurley, D. P. Costa, Maneuverability by the sea lion *Zalophus californianus*: Turning performance of an unstable body design. *J. Exp. Biol.* **206**, 667–674 (2003).
46. A. J. Werth, M. M. Kosma, E. M. Chenoweth, J. M. Straley, New views of humpback whale flow dynamics and oral morphology during prey engulfment. *Mar. Mamm. Sci.* **35**, 1556–1578 (2019).
47. A. James, T. Probyn, The relationship between respiration rate, swimming speed and feeding behaviour in the Cape anchovy *Engraulis capensis* Gilchrist. *J. Exp. Mar. Biol. Ecol.* **131**, 81–100 (1989).
48. M. A. Gil, A. M. Hein, Social interactions among grazing reef fish drive material flux in a coral reef ecosystem. *Proc. Natl. Acad. Sci. U.S.A.* **114**, 4703–4708 (2017).
49. D. Lavoie, Y. Simard, F. J. Saucier, Aggregation and dispersion of krill at channel heads and shelf edges: The dynamics in the Saguenay-St. Lawrence marine park. *Can. J. Fish. Aquat. Sci.* **57**, 1853–1869 (2000).
50. E. Jourdain, D. Vongraven, Humpback whale (*Megaptera novaeangliae*) and killer whale (*Orcinus orca*) feeding aggregations for foraging on herring (*Clupea harengus*) in Northern Norway. *Mamm. Biol.* **86**, 27–32 (2017).
51. M. E. Fournet, C. M. Gabriele, F. Sharpe, J. M. Straley, A. Szabo, Feeding calls produced by solitary humpback whales. *Mar. Mamm. Sci.* **34**, 851–865 (2018).
52. T. Leighton, D. Finfer, E. Grover, P. White, An acoustical hypothesis for the spiral bubble nets of humpback whales, and the implications for whale feeding. *Acoust. Bull.* **32**, 17–21 (2007).
53. R. Mills, H. Hildenbrandt, G. K. Taylor, C. K. Hemelrijk, Physics-based simulations of aerial attacks by peregrine falcons reveal that stooping at high speed maximizes catch success against agile prey. *PLOS Comput. Biol.* **14**, e1006044 (2018).
54. P. S. Segre *et al*., Hydrodynamic properties of fin whale flippers predict maximum rolling performance. *J. Exp. Biol.* **219**, 3315–3320 (2016).
55. M. Bejder, D. W. Johnston, J. Smith, A. Friedlaender, L. Bejder, Embracing conservation success of recovering humpback whale populations: Evaluating the case for downlisting their conservation status in Australia. *Mar. Policy* **66**, 137–141 (2016).
56. V. J. D. Tulloch, É. E. Plagányi, C. Brown, A. J. Richardson, R. Matear, Future recovery of baleen whales is imperiled by climate change. *Glob. Change Biol.*, 10.1111/gcb.14573 (2019).

Downloaded at STANFORD UNIV MED CENTER on December 23, 2019